Journal of Geography and Cartography 2024, 7(2), 7981.
https://doi.org/10.24294/jgc7981

Article

A remote sensing approach to identify environmental economics considering blue carbon sequestration in Satkhira coastal area, Bangladesh

Raiyan Siddique[1], M. R. Ashikur[2,*], Taspiya Hamid[1], Mohammad Azharul Islam[1]

[1] Department of Oceanography & Hydrography, Bangabandhu Sheikh Mujibur Rahman Maritime University, Dhaka 1216, Bangladesh
[2] Institute of Bay of Bengal & Bangladesh Studies, Bangabandhu Sheikh Mujibur Rahman Maritime University, Dhaka 1216, Bangladesh
*** Corresponding author:** M. R. Ashikur, ro.ibbbs@bsmrmu.edu.bd

CITATION

Siddique R, Ashikur MR, Hamid T, Islam MA. A remote sensing approach to identify environmental economics considering blue carbon sequestration in Satkhira coastal area, Bangladesh. Journal of Geography and Cartography. 2024; 7(2): 7981. https://doi.org/10.24294/jgc7981

ARTICLE INFO

Received: 15 July 2024
Accepted: 22 October 2024
Available online: 8 November 2024

Abstract: The persistence of coastal ecosystems is jeopardized by deforestation, conversion, and climate change, despite their capacity to store more carbon than terrestrial vegetation. The study's objectives were to investigate how spatiotemporal changes impacted blue carbon storage and sequestration in the Satkhira coastal region of Bangladesh over the past three decades and, additionally to assess the monetary consequences of changing blue carbon sequestration. For analyzing the landscape change (LSC) patterns of the last three decades, considering 1992, 2007, and 2022, the LSC transformations were evaluated in the research area. Landsat 5 of 1992 and 2007, and Landsat 8 OLI-TIRS multitemporal satellite images of 2022 were acquired and the Geographical Information System (GIS), Remote Sensing (RS) techniques were applied for spatiotemporal analysis, interpreting and mapping the output. The spatiotemporal dynamics of carbon storage and sequestration of 1992, 2007, and 2022 were evaluated by the InVEST carbon model based on the present research years. The significant finding demonstrated that anthropogenic activity diminished vegetation cover, vegetation land decreased by 7.73% over the last three decades, and agriculture land converted to mariculture. 21.74% of mariculture land increased over the last 30 years, and agriculture land decreased by 12.71%. From 1992 to 2022, this constant LSC transformation significantly changed carbon storage, which went from 11706.12 Mega gram (Mg) to 9168.03 Mg. In the past 30 years, 2538.09 Mg of carbon has been emitted into the atmosphere, with a combined market worth of almost 0.86 million USD. The findings may guide policymakers in establishing a coastal management strategy that will be beneficial for carbon storage and sequestration to balance socioeconomic growth and preserve numerous environmental services.

Keywords: remote sensing; geographical information system; InVEST carbon model; blue carbon storage and sequestration; environmental economics

1. Introduction

Carbon is sequestered by coastal ecosystems such as mangroves and seagrass meadows at rates that are substantially greater per unit area in comparison to terrestrial vegetation [1]. Coastal habitats have been identified as having some of the most concentrated quantities of carbon on the planet [2]. Several studies reveal that mangrove ecosystems typically absorb an average of 6 to 8 Mega gram (Mg) of Carbon dioxide (CO_2) per hectare of carbon annually (tons of CO_2 equivalent per hectare) [3]. The carbon sequestration process of an ecosystem absorbs and retains more carbon in biomass, sediments, or water than is released into the atmosphere [4]. Recent research into the function of blue carbon throughout the global carbon cycle indicates that coastal habitats not only encompass enormous above-ground biomass on tropical shorelines but also possess considerably more below-ground carbon storage [5]. Blue

carbon, in contrast to green carbon that exists in terrestrial vegetation, endures in ocean sediments for thousands of years [6].

Blue carbon sequestration (BCS) employs the carbon-sequestration competencies of marine creatures and coastal ecosystems to establish carbon sinks. The extraction and processing of blue carbon (BC) could evolve into a financially sustainable industrial endeavor, stipulating the fact that an internationally recognized trading market has been established and a feasible measurement and valuing system for carbon sink services has been placed in established [7]. The efforts intended for restoring and protecting BC also offer the potential to develop market-driven mechanisms that exploit existing frameworks for carbon offsets (also called carbon credits). The commercial viability of BC extraction and processing would be attained through the establishment of a global trading market and the implementation of a proper measurement and pricing mechanism for carbon sink commodities [8].

Coastal habitats are widely regarded as some of the most ecologically and economically crucial regions on Earth [6]. Coastal environments offer a diverse range of amenities and goods [9]. The natural processes and components of ecosystems that contribute to human demands for commodities and amenities are known as ecosystem services [10]. Coastal habitats offer vital ecosystem services due to their variety of ecosystems and organisms that serve a crucial role in preserving the carbon cycle's equilibrium [11]. Bangladesh's coastal and marine ecosystems are integral to the Bay of Bengal (BoB) large marine ecosystems (LMEs), one of 64 LMEs worldwide. A substantial proportion of people living in Bangladesh's coastal region and elsewhere depend on ecosystem services from the coastal and marine ecosystem for their livelihoods and income. The same argument applies to several coastal communities across the globe as well [12]. The Blue Economy (BE) entails a range of commercial activities, goods, services, and investments that hinge on and have an impact on coastal and marine resources [13]. The two primary anthropogenic stresses that coastal ecosystems face worldwide are urbanization and industrialization and these two factors influence the intensity of landscape change (LSC) and have altered the coastal land cover in recent decades [14]. The structure and zonation of the coastal environment have been greatly disturbed by coastal disturbances and changes in LSC [15]. When attempting to comprehend and simulate the transformation in the coastal regions of the planet, LSC modification is considered to be one of the most vital processes. Complex interconnections between human and environmental driving variables are what cause it [16]. BC habitats are threatened by anthropogenic activities such as land conversion for agricultural production and urban growth [17]. The FAO's worldwide forest resources evaluation for 2020 revealed that 113 nations and territories possess mangrove forest lands. From 1990 to 2020, there was a global decline of 1.04 million hectares in the mangrove area [18].

There are a multitude of conventional methods for quantifying stored carbon. The estimation and assessment of spatially explicit services for carbon sequestration potential might vary depending on factors such as meteorological conditions, management applications, ecosystem characteristics, species composition, and local populations. When applied to individual foundational issues, the combination of geographic information systems (GIS) and remote sensing (RS) will produce the most reliable results [19]. A method for tracking the spatiotemporal distribution and

condition of coastal ecosystems is RS [20]. Utilizing four carbon pools, the concept of the InVEST Carbon model is used to estimate the current carbon stocks and their potential future growth (aboveground biomass, underground biomass, dead organic matter, and soil carbon) [16]. The InVEST blue carbon model evaluates the fluctuating value of carbon storage and sequestration services provided by coastal ecosystems. It performs this by analyzing the variations in carbon storage over a specific timeframe and contrasting them with various management scenarios.

Ma et al. 2019 have investigated the storage of coastal blue carbon in the Yellow River Delta and its relationship to changes in land cover over the previous four decades in their study article [21]. Aljenaid et al. 2022 have combined GIS and RS data for evaluating the spatiotemporal changes of mangroves in Bahrain over the last 50 years and their relationship with carbon stocks and potential emissions [6].

Climate change is characterized by rising sea levels, increased salinity, and a higher frequency of cyclones making the Satkhira region vulnerable. These environmental stresses and anthropogenic activity put at risk local ecosystems, including the mangrove forests of the Sundarbans, while diminishing the carbon sequestration capacity of these essential blue carbon ecosystems. Despite these challenges, the Satkhira region presents considerable opportunities for blue carbon sequestration. The Sundarbans, recognized as the largest mangrove forest globally, provide significant carbon storage potential. Regional conservation and restoration efforts, supported by government and international organizations, can improve blue carbon sequestration. The increasing global interest in carbon credits offers an economic motivation for the preservation of these ecosystems. Carbon offset programs could fund Satkhira conservation while mitigating climate change and protecting biodiversity.

This study contributes to existing research on blue carbon by examining the environmental economics of BCS rates in the Satkhira coastal area of Bangladesh and specifically reviews earlier studies that mostly focused on data collection and the mapping of blue carbon ecosystems in different nations. In this study, the LSC intensity over the past three decades in the study area using the GIS and RS techniques to better understand the issue. This study's main objectives are to investigate how spatiotemporal changes impact blue carbon storage and sequestration in the research area over the last three decades and evaluate shifting BCS from an economic angle.

2. Materials and methods

2.1. Study area

Satkhira, located in the Southwestern region of Bangladesh, is a constituent of the Khulna division. The Satkhira district has boundaries set by the Jashore district to the North, the Khulna district to the East, the BoB to the South, and India to the West. It is located between latitudes 21°36' North and 22°54′ North and longitude 88°54′ East and 89°20′ East (**Figure 1**). The district has 1440 villages, 2 paurashavas, 7 upazilas, 79 unions, 953 mauzas, 18 wards, and 42 mahallas. Satkhira Sadar, Assasuni, Debhata, Kalaroa, Kaliganj, Shyamnagar, and Tala are the upazilas of the Satkhira district [22]. According to the Bangladesh Meteorological Department (BMD) in 2022, Satkhira's yearly average temperature is 77.0° F (25 ℃). May is considered the highest

average temperature, at 86.0° F (30 °C). January has the lowest average temperature, at 66.0° F (18.9 °C). In Satkhira, there are 66.5 inches (1689.1 mm) of precipitation on average each year. With 13.9 inches (353.1 mm) of precipitation on average and July is the month with the most precipitation. January has an average of 0.3 inches (7.6 mm) of precipitation, making it the month with the least amount [23]. The important rivers in this region include the Kobadak, Sonai, Kholpatua, Morischap, Raimangal, Hariabhanga, Ichamati, Betrabati, etc. [24].

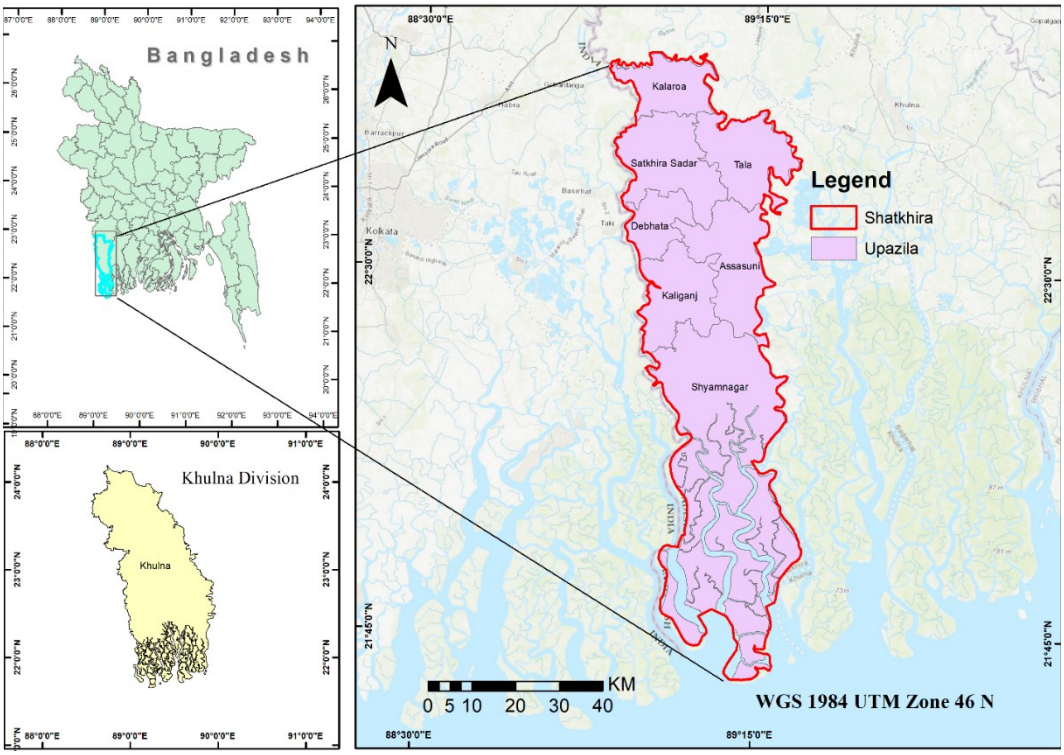

Figure 1. Map shows the location of the study area, index map shows Bangladesh and Khulna division.

2.2. Overview of data and pre-processing

Landsat 4–5 Thematic Mapper (TM) level one image for 1992, 2007 and Landsat 8 OLI/TIRS images for 2022 were acquired from the United States Geological Survey (USGS) for the detection of LSC alteration of the area of interest (AOI). Nine satellite images from the same month of March with a 15-year interval were collected from the USGS. The characteristics and information of the research data are given in **Table 1**.

Table 1. Description of the data used for this study.

Year	Date of Acquisition (yr-mm-dd)	Sensor	Path	Row	Resolution	Cloud Cover
1992	1992-03-08	TM	138	$\frac{44}{45}$	30 m	<10%
2007	2007-03-08	TM	138	$\frac{44}{45}$	30 m	<10%
2022	2022-03-03	OLI_TIRS	138	$\frac{44}{45}$	30 m	<10%

The susceptibility of Landsat sensor-captured images to distortion was influenced by elements such as sensors, solar conditions, atmospheric conditions, and topography.

Preprocessing made a concerted attempt to minimize these effects to the greatest extent possible for a specific application [25]. The satellite images were selected based on several criteria (1) The satellite images must have cloud coverage of less than 10% over the whole research region, or ideally, be completely free of clouds. (2) It is essential to provide access to a continuous sequence of Landsat images over a significant period to optimize the distinction and categorization of diverse land utilization patterns [26]. According to Koppen's climate zone, the Satkhira coastal area was situated in a tropical climate zone [27]. Obtaining completely free cloud data is indicated to be quite challenging. Nevertheless, the data collected for this study only had minimal cloud coverage, amounting to less than 10%. The haze and clouds in satellite images were effectively eliminated using Erdas Imagine software v14.

Due to the absence of homogeneity in the time series of Satellite images, it was necessary to evaluate abrupt changes in the LSC while utilizing multi-temporal satellite images. The noise from surface signals, as well as the absorption and scattering of atmospheric gases and aerosol particles as they passed through the earth's atmosphere and back to the sensor, had an impact on this homogeneity. The satellite images may be accurately interpreted due to atmospheric influences. The atmospheric impact should be removed from the satellite images during pre-processing in order to evaluate change detection [28].

The essential process for transforming image data from many sensors and platforms into a physically significant common radiometric scale was the calculation of at-sensor spectral radiance. Using 32-bit floating-point calculations, pixel values (Q) from unprocessed, raw data were changed into absolute spectral radiance units during radiometric calibration. The Equation (1) was carried out to perform the Q_{cal}-to-L_λ conversion for Level 1 products [26, 28–30].

$$L\lambda = \left(\frac{LMAX\lambda - LMIN\lambda}{Qcalmax - Qcalmin}\right)(Qcal - Qcalmin) + LMIN\lambda \quad (1)$$

where;

L_λ = Spectral radiance at the sensor's aperture [W/ (m^2 sr μm)]

Qcal = Quantized calibrated pixel value [DN]

Qcalmin = Minimum quantized calibrated pixel value corresponding to $LMIN\lambda$ [DN]

Qcalmax = Maximum quantized calibrated pixel value corresponding to $LMAX_\lambda$ [DN]

$LMIN_\lambda$ = Spectral at-sensor radiance that is scaled to *Qcalmin* [W/(m^2 sr μm)]

$LMAX_\lambda$ = Spectral at-sensor radiance that is scaled to *Qcalmax* [W/(m^2 sr μm)]

By converting the at-sensor spectral radiation to exo-atmospheric TOA reflectance, sometimes referred to as in-band planetary albedo, was achieved scene-to-scene variability. There were three benefits to employing TOA reflectance instead of at-sensor spectral radiance when comparing images from various sensors. The cosine impact of varied solar zenith angles caused by the delay in data collecting is first eliminated. The second was that TOA reflectance made up for variations in exo-atmospheric solar irradiance caused by spectral band discrepancies. Third, the fluctuation in the earth-sun distance between several data-gathering dates was adjusted for using the TOA reflectance. These changes had a big impact on time and space, too.

The acquired value of radiance was converted to top of the atmosphere (TOA) reflectance, which was how the earth's TOA reflectance was calculated from Equation (2) [31].

$$\rho = \frac{\pi L\lambda d^2}{ESUN\lambda . \cos\theta s} \quad (2)$$

where;

ρ = Planetary TOA reflectance for δ [unitless]

π = Mathematical constant equal to~3.14159 [unitless]

$L\lambda$ = Spectral radiance at the sensor's aperture [W/(m^2 sr μm)]

d = Earth–Sun distance [astronomical units]

$ESUN\lambda$ = Mean exo-atmospheric solar irradiance [W/(m^2 μm)]

θs = Solar zenith angle [degrees]

ArcGIS software v10.5 was used to process radiometric calibration, radiometric correction, image cropping, and mapping.

2.3. LSC classification

Multiband raster images with LSC data extracted by classification and image analysis. Autonomously grouping pixels with comparable reflectance ranges into a specific LSC class was the objective of both supervised and unsupervised image classification. Supervised classification, a method directed by the user, entails the selection of training sites to serve as references for categorization. Supervised classification was implemented using a variety of methods, including parallelepiped classification, K-nearest neighbor, minimal distance classification, and others [32].

The commonly used maximum likelihood classification method was applied to the LSC classification in this study using ArcGIS software. The spectral response patterns' variance and covariance were quantitatively evaluated by the maximum likelihood algorithm, and each pixel was then assigned to the class with the greatest likelihood of association [32].

Six LSC categories were selected in total: water body, tide flat, mariculture, built-up area, vegetation, and cultivated land (**Table 2**). For each of the LSC classes, about 50 training samples were gathered for maximum likelihood classification. To estimate the LSC change, multitemporal raster layers were created, and their corresponding data were compared.

Table 2. The classification method for LSC employed in this study.

LSC categories	Description
Built-up Area	Residential; commercial and services; transportation infrastructure; industrial; mixed urban and other urban
Cultivated Land	Agriculture land; paddy field; vegetables; fruits; and other cultivated lands
Water Body	River; canal; pond; Permanent open water; lakes
Mari culture	Shrimp aquaculture; Gher
Vegetation	Mangrove vegetation; homestead vegetation; urban vegetation
Tidal flat	Deposit mud or sand; coastal wetlands

2.4. Accuracy assessment

Three distinct accuracy assessments were conducted to evaluate the quality of the generated LSC map. The error matrix technique was used for the initial approach. The integration of reference data and independent categorization allowed for a clear comprehension of the situation in the field [33]. Accuracy identified the degree to which the created map agreed with the reference categorization. The correctness of a study was frequently assessed using the Kappa coefficient of agreement. Kappa was said to include a correction for "random allocation agreement". By using Equation (3) the Kappa coefficient was calculated [32,34].

$$\text{Kappa coefficient (K)} = \frac{n\sum_{i=1}^{r} x_{ii} - \sum_{i=1}^{r} x_i + x + i}{n^2 - \sum_{i=1}^{r} x_i + x + i} \quad (3)$$

Here;

x_{ii} is the number of observations in row i and column i;

$x_i +$ and $x + i$ are marginal totals for row i and column i respectively;

n is the total number of observations (pixels)

Through the creation of an error matrix; the accuracy of each raster layer was evaluated in the current study. Stratified random sampling was used for the accuracy evaluation. Overall accuracy was calculated by using the Equation (4) [32,34].

$$\text{Overall accuracy } = \frac{\sum_{i=1}^{r} x_{ii}}{x} \quad (4)$$

where x_{ii} is the diagonal elements in the error matrix;

x is the total number of samples in the error matrix; and r is the number of rows in the matrix.

2.5. Blue carbon storages and sequestration utilizing the InVEST carbon model

The quantity of static carbon storage and dynamic sequestration for each cell in the research area was calculated using the InVEST 3.10.2 carbon model. The four carbon pools were examined in this module: soil organic carbon, belowground carbon density, aboveground carbon density, and dead organic matter. The calculation of the carbon storage $C_{m;I;j}$ in a given grid cell (i; j) with land use type "m" achieved by Equation (5) [35].

$$C_{m;I;j} = A \times (Ca_{m;I;j} + Cb_{m;I;j} + Cs_{m;I;j} + Cd_{m;I;j}) \quad (5)$$

In this formula, A is the real area of each grid cell (ha).

$Ca_{m;I;j}$; $Cb_{m;I;j}$; $Cs_{m;I;j}$ $Cd_{m;I;j}$ are the aboveground carbon density, belowground carbon density, soil organic carbon density, and dead organic matter carbon density (i; j), respectively.

Finally, carbon storage "C" and carbon sequestration "S" were calculated by Equations (6) and (7) for the whole case study region [35].

$$C = \sum_{m=1}^{n} c_{m;i;j} \quad (6)$$

$$S = C^{T2} - C^{T1} \quad (7)$$

In Equation (7), C^{T2} and C^{T1} demonstrate static carbon storage in years T2 and T1 (here T2 > T1). The needed data for running the carbon storage model was the LSC map and the biophysical table containing columns of LSC, '*C*_above' '*C*_below' '*C*_soil,' and '*C*_dead' (**Table 3**).

Table 3. Types of LSC and the elements that make up their carbon pools [21,35,36].

LSC Type	C_above (Mg/hm^2)	C_below (Mg/hm^2)	C_soil (Mg/hm^2)	C_dead (Mg/hm^2)
Vegetation	14	7	15	1
Water Body	2	1	10	0
Tidal Flat	6	2	16	1
Mari culture	1	0	12	0
Built-up Area	0	0	8	0
Agriculture Land	4	9	25	1

C_above = Above ground carbon biomass; C_below = Below ground carbon biomass; C_soil = Soil carbon biomass; C_dead = Dead carbon biomass.

The InVEST model, although commonly employed for ecosystem service valuation. The model relies significantly on the quality of input data, which encompasses LSC maps, vegetation characteristics, and various biophysical parameters. Inaccuracies in these inputs can propagate through the model, resulting in potential errors in estimating ecosystem services, such as carbon storage.

2.6. Economic evaluation of blue carbon sequestration

The final step assessed the economic value of BCS in the Satkhira shoreline region. Over 30 years, the LSC in the research region changed, resulting in a modification of the storage of blue carbon. The rate of carbon sequestration was also altered due to the shift in storage. Unfortunately, the Satkhira region did not have any long-term information on the societal costs of land-use change, particularly the removal of mangrove forests and other vegetation. The monetary value of blue carbon across the Satkhira region was calculated based on estimates of the social cost of carbon and the current price of carbon credits. Hence, the economic data about the cost of carbon per mega gram was derived from several sources, including research studies and international organizations, to analyze and assess the economic significance of carbon. The price of carbon at the moment around $50 per Mg [37]. In this study, the carbon cost was set at $50 per Mg.

3. Results and discussion

3.1. Spatial and temporal transformation of LSC

The RS technology illustrated the LSC dynamics of the Satkhira shoreline area from 1992 to 2022. The spatial and temporal distribution of LSC patterns considered six classes and these were tidal flat, vegetation, water body, mariculture, agriculture land, and built-up area as shown in **Figure 2**. The percentage of different LSC classes and their percentage of cover change in the years 1992, 2007, and 2022 are presented

in **Table 4**. The tidal flat regions have consistently dropped over the years, with a decline from 9.34% in 1992, to 8.2% in 2007, and further down to 6.07% in 2022. Conversely, the vegetation in the study region rose from 33.11% in 1992 to 41.1% in 2007 but declined to 25.39% in 2022. On the other hand, agricultural land areas experienced a significant decrease from 20.92% in 1992 to 4.93% in 2007, followed by a rise in 2022 to 8.21%. Also, build-up areas reduced from 22.29% in 1992 to 17.2% in 2007, followed by a rise in 2022 to 23.65%. Mari culture areas continued their increasing trend from 1992, 2007, and 2022 where it increased from 6.25% to 27.99% respectively. Eventually, there was an absence of discernible alterations in the aquatic systems within the designated research region. The aquatic ecosystem had a 0.61% increase in size during the previous 30 years.

Table 4. Percentile of the LSC categories and percentile change between the study years 1992; 2007; and 2022.

	Percentile (%)			**Percentile change**		
Class Name	1992	2007	2022	2007–1992	2022–2007	2022–1992
Tidal Flat	9.34	8.20	6.07	−1.14	−2.13	−3.27
Vegetation	33.11	41.10	25.39	7.98	−15.71	−7.73
Water Body	8.08	8.04	8.69	−0.03	0.65	0.61
Mari culture	6.25	20.52	27.99	14.27	7.47	21.74
Agriculture Land	20.92	4.93	8.21	−15.98	3.28	−12.71
Built-up Area	22.29	17.20	23.65	−5.09	6.45	1.36

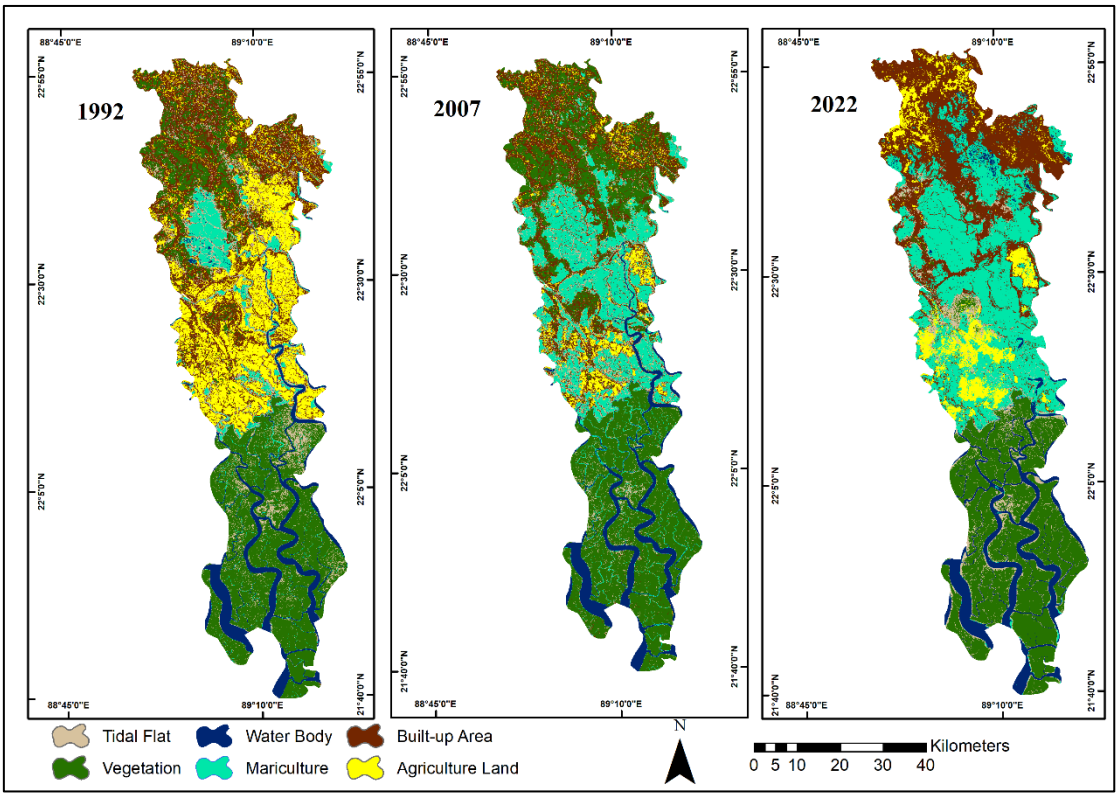

Figure 2. Land cover changes over time in 1992, 2007, and 2022.

Over the past three decades, tidal flats deteriorated by around 4%, with uneven patterns in vegetation cover. The vegetation rose in 2007 as a result of various

afforestation efforts, but by 2022 the rapid growth of urbanization, unplanned development, and various socioeconomic activities reduced the vegetation land cover by approximately 8%. The class demonstrated a linear relationship between the years, water bodies did not alter significantly. One of the top nations in the world for shrimp production is Bangladesh. The majority of the coastal population makes a living by raising shrimp. As a result, the area used for mariculture rapidly increased. The research area forecasted a growth of over 22% in this class during the past thirty years. Since the majority of agricultural land was converted to mariculture, the rapid expansion of mariculture land led to the degradation of agricultural land. During the research period, agricultural land declined by about 13%. Additionally, the built-up area grew by about 2%. The main factors related to the increasing development of land use at the expense of deteriorating the vegetation covers can be attributed to urban expansion.

3.2. The estimation of blue carbon storages and sequestration

3.2.1. The changes in carbon pool value

In the research area, significant land cover altered over the past 30 years resulted in a substantial change in CO_2 levels. Four carbon pools were affected by the LSC transition. The spatiotemporal changes of carbon pool value are presented in **Figure 3**. **Table 5** displays the summary of the changes in carbon pool value due to the alteration of LSC in Satkhira between 1992 and 2022. Overall, the carbon pool value changed significantly within the period where carbon below value (BBC), carbon dead value (DOM), and carbon soil value (SOC) reduced in considerable amount with noticeable fluctuation in carbon above value (ABG). ABG showed rising from 1992 to 2007 with a considerable decline in 2022. Over the past 30 years, DOM did not shift that much in the Satkhira coastline region with little change in the CO_2 value. DOM ranged between 1992 and 2022 from 322.92 Mg to 201.87 Mg.

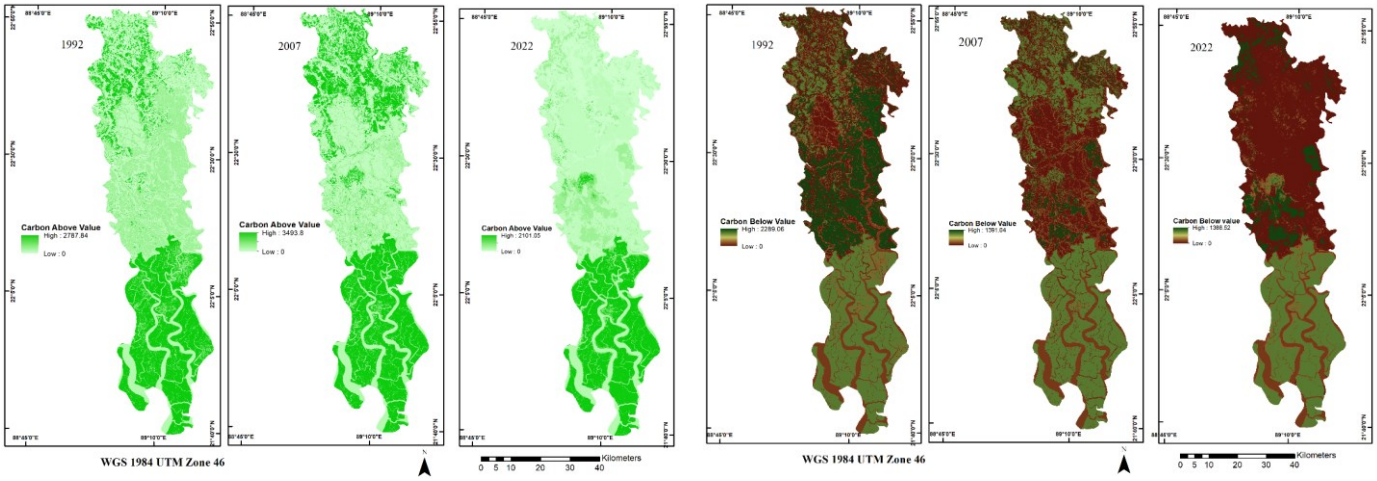

(a) **(b)**

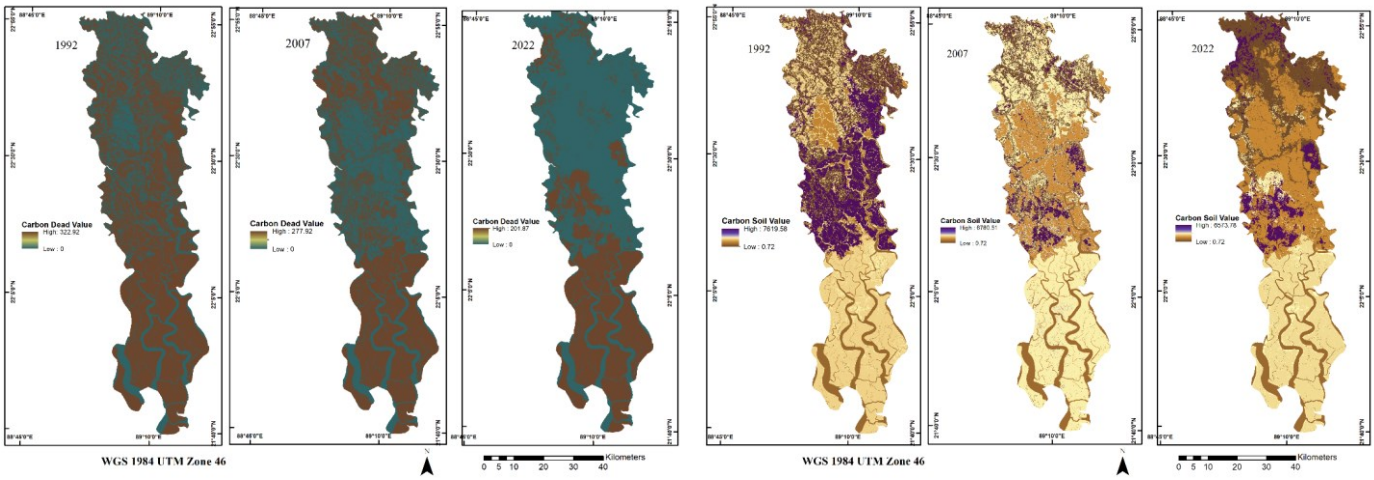

(c) **(d)**

Figure 3. Spatiotemporal changes of carbon pool value. **(a)** ABG, **(b)** BBC, **(c)** DOM, **(d)** SOC.

Table 5. The threshold for the amount of carbon ABG, BBC, DOM, SOC value (Mg) in the soil changed during the study.

CATEGORY	1992	2007	2022
(A) ABG	2787.84	3493.8	2101.05
(B) BBC	2289.06	1388.52	1391.04
(C) DOM	322.92	277.92	201.87
(D) SOC	7619.58	6780.51	6573.78

3.2.2. Calculation of blue carbon storages and sequestration

The spatial distribution of carbon storage variation in the study area is depicted in **Figure 4**. The Satkhira coastline region stored 11706.12 Mg of carbon in total in 1992. The value of the carbon stored was downgraded in 2007, the value of carbon stored in 2007 was 10779.84 Mg. The most concerning outcome was in 2022 when Satkhira's carbon stored capacity was downgraded to the largest amount of 9168 Mg. The highest carbon storage capacity was found in mangrove vegetation and carbon storage was minimal in the built-up area**.** The vegetation contributed the largest amount C for the total value of the ecosystem. Also, it revealed low carbon in water bodies. Thus, the study suggested conserving the mangrove vegetation for sustaining carbon storage.

The second output of this model was the calculation of CS. The values of CS came to negative ranges. The negative values indicated lost carbon; indicated sequestered carbon in Mg per pixel. **Figure 5** depicts the comparison of carbon storage and sequestration in the research area throughout the study period. As carbon storage facilities degraded over the last three decades. CS rates also declined. CS differences between the years were obtained from **Table 6**. It showed that in 2007–1992; CS rates were higher than the difference between 2022–2007 and 2022–1992. **Table 6** shows CS changing with 15-year intervals. Between 2007–1992 CS was found −926.28 Mg. CS rates were found to continuously degrade next 15 years interval which was from 2022 to 2007 –1611.81 Mg carbon was emitted into the atmosphere between this time frame. Overall last 30 years interval from 1992–2022. CS degradation intensity rose

at an alarming rate. In this study; it was estimated that CS degraded almost −2538.09 Mg; nearly a 27.68% reduction compared with the previous research year.

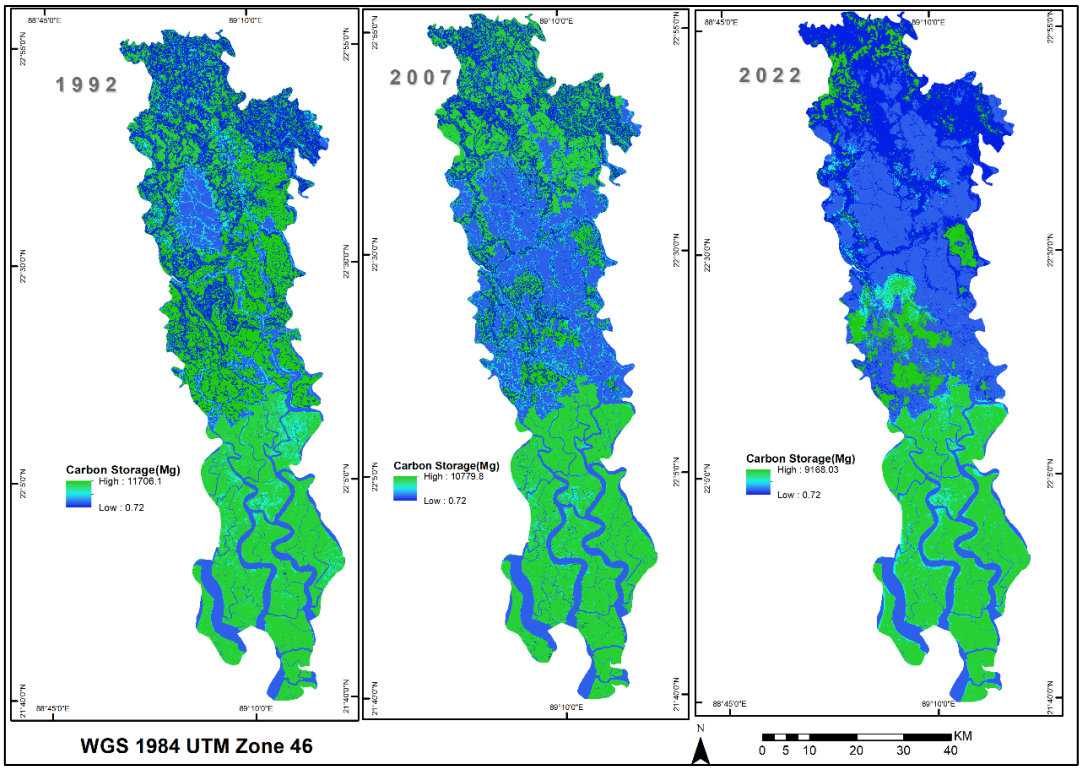

Figure 4. Changes in total carbon storage from 1992, 2007, and 2022, respectively, in the study area.

Table 6. Comparison of carbon sequestration in the different study years.

Category	2007–1992	2022–2007	2022–1992
(a) Carbon sequestration (Mg)	−926.28	−1611.81	−2538.09
(b) Carbon sequestration changes in (%)	−8.59%	−17.58%	−27.68%

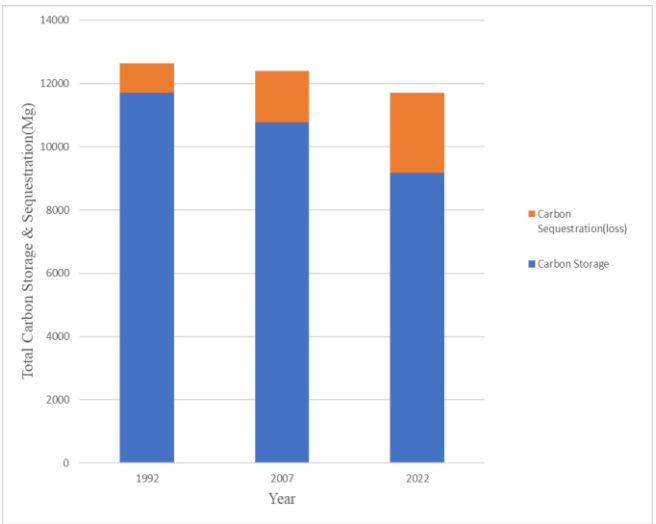

Figure 5. Changes in carbon storage and sequestration comparison chart.

3.3. Economic evaluation of reducing BCS

The outcome of the carbon model was the allocation of economic value for carbon sequestration over several years. The findings of this study indicated that the coastal environment has degraded over the last three decades. The coastal environment deteriorated due to a combination of natural and human activities. As a result, the level of BCS experienced a major decline, while there was a considerable increase in carbon emissions. The blue carbon storage and sequestration calculation section showed that the landscape of the Satkhira district changed very rapidly, approximately 2538.09 Mg of carbon was degraded over the last 30 years, indicating that carbon was not stored but emitted into the atmosphere in the research area. According to **Table 7**, a large amount of carbon was cast into the atmosphere every decade, with a market value of around 0.86 million USD per Mg. During 2007–1992, the carbon emitted into the atmosphere was 926.28 Mg, with a market value of about 0.046 million USD. During 2022–2007, the carbon emitted into the atmosphere was 1611.81 Mg, of which carbon credit was around 0.86 million USD. Due to its low carbon emissions compared to other wealthy countries, which had high carbon emission levels, Bangladesh could continue to profit from carbon trading. The coastal carbon ecosystem was found considerable changes, per the study, changed over the past three decades. The carbon sequestration rate significantly decreased, and a considerable amount of carbon was released into the atmosphere.

Table 7. Economic validation of carbon sequestration during the study year (unit is in million USD).

Category	2007−1992	Carbon Credit	2022−2007	Carbon Credit	2022−1992	Carbon Credit
Carbon Sequestration (Mg)	−926.28	0.046	1611.81	0.80	2538.09	0.86

3.4. Cumulative transformation between LSC and blue carbon dynamics

Integrating land use scenarios and the InVEST model could make it easier to assess the spatial and temporal effects of LSC on carbon storage and sequestration at the landscape scale This study explored the effects and causes of linkage in blue carbon dynamics concerning LSC transformation. From **Table 3**, it was noticed that each LSC class had a different carbon content value. Vegetation had the highest ABG carbon value. As a result, the most abundant ABG stock was found in vegetation areas. According to **Table 4**, vegetation rates increased in 2007. ABG was found to be high in 2007 in comparison with 1992, and 2022 (**Table 5**). So, this changing LSC class area ultimately affected the carbon value. This shifting of LSC caused the alteration of carbon pool value, and these changing pool values affected the carbon storage and sequestration in the research area. **Table 5** shows that SOC changed throughout the study year. This changing SOC value was related to the alteration of agricultural land. Agriculture land could store the highest amount of carbon soil biomass. This study provided information that agricultural land declined quickly in the research area. As a result, it was found that SOC continuously degraded in the Satkhira coastal region. The most alarming alteration of carbon value was seen with the alteration of vegetation land cover. Vegetation had not only the highest ABG value along with agriculture but also the highest BBC carbon value. BBC Carbon value in the Satkhira degraded last three decades because it related to vegetation and agricultural land. From the temporal

distribution of these two LSC classes, it was observed that these two LSC classes had a cumulative relation with the carbon pool value, which degraded the SOC value. This study provided a clear overview of blue carbon dynamics and how they are influenced by LSC transformation.

Aljenaid et al. [6] 2022 utilized GIS and RS data to analyze spatiotemporal changes in mangrove habitat. Their findings indicated that Tubli Bay has undergone considerable human activity starting in the 1960s, which ultimately led to the clearing of mangroves. Consequently, the carbon stored in the mangrove environment decreased by 85 from 34, 932 Mg C/ha in 1967 to 5, 112 Mg/ha in 2020. As a result, with an average of 9874.62 Mg CO_2 e yr^{-1} over the previous 53 years, the potential for carbon sequestration grew from 128,200.44 Mg CO_2 e ha^{-1} in 1967 to 18,761.04 Mg CO_2 e ha^{-1} in 2020 [6].

Ma et al. [21] 2019 presented that their study's main purpose was to investigate how land cover changes affect the spatiotemporal dynamics of coastal blue carbon sequestration considering various human-induced and natural driving processes. Their key findings were a 78% loss in shrub and forest cover between 1970 and 2010 and a 1.63×10^6 Mg decline in coastal blue carbon sequestration [21].

3.5. Accuracy assessment

In this study total three accuracy assessments were followed overall accuracy, kappa coefficients, and confusion matrix. Google earth pro was used for validation to assess the accuracy. 40 samples were taken from each LSC class and compared to classified data in the confusion matrix. For study years 1992, 2007, and 2022, the confusion matrix was used to represent producer accuracy and user accuracy, respectively. The Kappa coefficient was adapted to measure the accuracy of classification, which could test all confusion matrix elements based on the minimum requirement. In the accuracy assessment, the identified categories of LSC needed to achieve the minimum requirements, which were at least 0.8. **Table 8** shows the validation for LSC in 1992, 2007, and 2022. Diagonal numbers indicate samples that were successfully categorized for each LSC class. The kappa coefficients for 1992, 2007, and 2022 are 0.84, 0.875, and 0.935, respectively. So, the identified categories of LSC were corrected because they achieved their minimum requirement, which was at least 0.8.

Table 8. Accuracy assessment table for LSC data obtained from Landsat imagery during study years.

Class	TF	V	W	M	A	BU	RT	UA (%)
a. Validation in 1992								
TF	35	2	3	0	0	0	40	87.5
V	0	36	0	0	4	0	40	90
W	2	0	34	4	0	0	40	85
M	0	0	2	34	1	3	40	85
A	0	0	0	3	37	0	40	92.5
BU	0	3	2	0	3	32	40	80
CT	37	41	41	41	45	35	240	

Table 8. (*Continued*).

Class	TF	V	W	M	A	BU	RT	UA (%)
PA (%)	94.59	87.8	82.93	82.93	82.22	91.43		
OA (%)	86.67%							
Kappa Coefficient(K)	0.84							
b. Validation in 2007								
TF	36	2	2	0	0	0	40	90
V	0	35	0	0	2	3	40	87.5
W	0	0	38	2	0	0	40	95
M	1	0	3	36	0	0	40	90
A	0	0	0	2	37	1	40	92.5
BU	0	5	0	0	2	33	40	82.5
CT	37	42	43	40	41	37	240	
PA (%)	97.23	83.33	88.37	90	90.24	89.19		
OA (%)	89.58							
Kappa coefficient (K)	0.875							
c. Validation in 2022								
TF	38	1	1	0	0	0	40	88.37
V	0	38	0	0	1	1	40	88.37
W	1	0	39	0	0	0	40	97.5
M	1	0	1	38	0	0	40	88.37
A	0	2	0	0	36	2	40	90
BU	0	1	0	0	1	38	40	95
CT	40	42	41	38	38	41	240	
PA (%)	88.37	90.48	95.12	100	94.74	92.68		
OA (%)	94.58							
Kappa coefficient (K)	0.935							

TF = Tidal flat; V = Vegetation; W = Water body; M = Mariculture; A = Agriculture land; BU = Built-up area; RT = Row total; UA = User's accuracy; PA = Producer's accuracy; OA = Overall accuracy.

4. Conclusion

The InVEST carbon model was used to estimate the storage and sequestration of blue carbon using the dynamic shift in LSC data of the Satkhira coastal region of Bangladesh. The findings showed how the fast loss of agricultural land, forest, and tidal flats harmed BCS and storage during the past three decades. This study found that carbon sequestration dropped by 27.68% in 2022 and blue carbon storage reduced from 11706.12 Mg to 9168.03 Mg between 2022 and 1992. Around 2538.09 Mg of carbon were released into the atmosphere in 2022. The total amount of carbon released into the atmosphere from 2022 to 1992 had a market worth of almost 0.86 million dollars (USD). This result gives essential input to policymakers regarding any development activities in the coastal area of Bangladesh. As a result, we have a modified LSC ecosystem that affects the blue carbon ecosystem. The ecological aspect and environmental sustainability must be considered before adopting any development activities, such that strategic position and ease of transit access are not the only

important considerations. Our research is anticipated to contribute vital information to understanding the dynamics of blue carbon storage and sequestration as these kinds of studies are being ignored in management and decision-making policy for the future of coastal ecosystems. This research also quantifies the economic value of carbon that is stored or emitted into the atmosphere. Quantifying the economic value of carbon is vital for the restoration of the blue carbon ecosystem. This collection of findings may offer the authorities a dynamic framework for systematic decision-making by considering the spatiotemporal variation in carbon storage and sequestration. This integrated strategy, which might be used to plan and manage the Satkhira coastal ecosystem, considers a variety of factors, including environmental preservation and sustainable development.

Author contributions: Conceptualization, RS and MRA; methodology, MRA; software, MRA; validation, RS and MRA; formal analysis and investigation, RS and MRA; resources, MRA; data curation, RS; writing—original draft preparation, RS; writing—review and editing, MRA, TH and MAI; visualization, TH and MAI; supervision, MRA; project administration, MRA; funding acquisition, MRA. All authors have read and agreed to the published version of the manuscript.

Funding: This research was funded by Bangabandhu Sheikh Mujibur Rahman Maritime University, Bangladesh (BSMRMU) through funding Code- PRMTTC 4829.

Acknowledgments: The authors thank to the US Geological Survey for assisting this research with data sets. The authors would also thank the IBBBS at BSMRMU; Bangladesh for delivering the software and lab assistance.

Conflict of interest: The authors declare no conflict of interest.

References

1. Bertram C; Quaas M; Reusch TBH; Vafeidis AT; Wolff C; Rickels W. The blue carbon wealth of nations. Nat Clim Chang. 2021;11(8):704-709. doi:10.1038/s41558-021-01089-4
2. Bindu G; Rajan P; Jishnu ES; Ajith Joseph K. Carbon stock assessment of mangroves using remote sensing and geographic information system. Egyptian Journal of Remote Sensing and Space Science. 2020;23(1):1-9. doi:10.1016/j.ejrs.2018.04.006
3. Harishma KM; Sandeep S; Sreekumar VB. Biomass and carbon stocks in mangrove ecosystems of Kerala; southwest coast of India. Ecol Process. 2020;9(1). doi:10.1186/s13717-020-00227-8
4. Taillardat P; Friess DA; Lupascu M. Mangrove blue carbon strategies for climate change mitigation are most effective at the national scale. Biol Lett. 2018;14(10). doi:10.1098/rsbl.2018.0251
5. Atchison J. Green and Blue Infrastructure in Darwin; Carbon Economies and the Social and Cultural Dimensions of Valuing Urban Mangroves in Australia. Urban Science. 2019;3(3):86. doi:10.3390/urbansci3030086
6. Aljenaid S; Abido M; Redha GK; et al. Assessing the spatiotemporal changes; associated carbon stock; and potential emissions of mangroves in Bahrain using GIS and remote sensing data. Reg Stud Mar Sci. 2022;52:102282. doi:10.1016/j.rsma.2022.102282
7. Zhao C; Fang C; Gong Y; Lu Z. The economic feasibility of Blue Carbon cooperation in the South China Sea region. Mar Policy. 2020;113(November 2019):103788. doi:10.1016/j.marpol.2019.103788
8. Steven ADL; Vanderklift MA; Bohler-Muller N. A new narrative for the Blue Economy and Blue Carbon. Journal of the Indian Ocean Region. 2019;15(2):123-128. doi:10.1080/19480881.2019.1625215
9. Jiezzelle V; Nesperos C; Mico C; Villanueva M; Garcia JE; Gevaña DT. Assessment of blue carbon stock of mangrove vegetation in Infanta; Quezon; Philippines. Ecosystems and Development Journal. 2021;11(1 and 2):48-60.

10. Carr EW; Shirazi Y; Parsons GR; Hoagland P; Sommerfield CK. Modeling the Economic Value of Blue Carbon in Delaware Estuary Wetlands: Historic Estimates and Future Projections. J Environ Manage. 2018;206:40-50. doi:10.1016/j.jenvman.2017.10.018
11. Sudirman N; Helmi M; Salim HL. Geospatial Modeling of Blue Carbon Ecosystem Coastal Degradation in Jakarta Bay. Indonesian Journal of Oceanography. 2019;1(1):80-92. doi:10.14710/ijoce.v1i1.6266
12. Islam MM; Shamsuddoha M. Coastal and marine conservation strategy for Bangladesh in the context of achieving blue growth and sustainable development goals (SDGs). Environ Sci Policy. 2018;87(12):45-54. doi:10.1016/j.envsci.2018.05.014
13. Whisnant; R. and AReyes. Blue Economy for Business in East Asia: Towards an Integrated Understanding of Blue Economy. Quezon City; Philippines: Partnerships in Environmental Management for the Seas of East Asia (PEMSEA). Published online 2015.
14. Sejati AW; Buchori I; Kurniawati S; Brana YC; Fariha TI. Quantifying the impact of industrialization on blue carbon storage in the coastal area of Metropolitan Semarang; Indonesia. Applied Geography. 2020;124(June):102319. doi:10.1016/j.apgeog.2020.102319
15. Walcker R; Gandois L; Proisy C; et al. Control of "blue carbon" storage by mangrove ageing: Evidence from a 66-year chronosequence in French Guiana. Glob Chang Biol. 2018;24(6):2325-2338. doi:10.1111/gcb.14100
16. Pechanec V; Purkyt J; Benc A; Nwaogu C; Štěrbová L; Cudlín P. Modelling of the carbon sequestration and its prediction under climate change. Ecol Inform. 2018;47(February):50-54. doi:10.1016/j.ecoinf.2017.08.006
17. Moritsch MM; Young M; Carnell P; et al. Estimating blue carbon sequestration under coastal management scenarios. Science of the Total Environment. 2021;777:145962. doi:10.1016/j.scitotenv.2021.145962
18. Pekkarinen A. Global Forest Resources Assessment 2020. Global Forest Resources Assessment 2020. Published online 2020. doi:10.4060/ca8753en
19. Giri RKKV; Mandla VR. Study and evaluation of carbon sequestration using remote sensing and GIS: A review on various techniques. International Journal of Civil Engineering and Technology. 2017;8(4):287-300.
20. Zheng Y; Takeuchi W. Quantitative assessment and driving force analysis of mangrove forest changes in china from 1985 to 2018 by integrating optical and radar imagery. ISPRS Int J Geoinf. 2020;9(9). doi:10.3390/ijgi9090513
21. Ma T; Li X; Bai J; Ding S; Zhou F; Cui B. Four decades' dynamics of coastal blue carbon storage driven by land use/land cover transformation under natural and anthropogenic processes in the Yellow River Delta; China. Science of the Total Environment. 2019;655:741-750. doi:10.1016/j.scitotenv.2018.11.287
22. Mahmud I; Mia AJ; Uddin R; Rahman M; Rahman MH. Assessment on Seasonal Variations in Waterlogging Using Remote Sensing and Gis Techniques in Satkhira District in Bangladesh. Barisal University Journal Part 1. 2017;4(1):67-80.
23. BMD. Temperature Data. Bangladesh Meteorological Department. 2022. https://www.bmd.gov.bd/
24. Islam SkM; Naher N; Roy N; Mahmud MdK; Hossain MdD; Modak S. Agricultural Adaptation Options against Adverse Effect of Climate Change in Shyamnagar Upazila in the Satkhira District; Bangladesh. Asian Journal of Research in Agriculture and Forestry. 2019;2(3):1-12. doi:10.9734/ajraf/2018/46438
25. Young NE; Anderson RS; Chignell SM; Vorster AG; Lawrence R; Evangelista PH. A survival guide to Landsat preprocessing. Ecology. 2017;98(4):920-932. doi:10.1002/ecy.1730
26. Sun Z; Ma R; Wang Y. Using Landsat data to determine land use changes in Datong basin; China. Environmental Geology. 2009;57(8):1825-1837. doi:10.1007/s00254-008-1470-2
27. Mahmud KH; Abid SB; Ahmed R. Development of a Climate Classification Map for Bangladesh Based on Koppen's Climatic Classification. 2018;XXXIX(June).
28. Tan KC; Lim HS; MatJafri MZ; Abdullah K. Landsat data to evaluate urban expansion and determine land use/land cover changes in Penang Island; Malaysia. Environ Earth Sci. 2010;60(7):1509-1521. doi:10.1007/s12665-009-0286-z
29. Ara S; Alif MAUJ; Islam KMA. Impact of Tourism on LSC and LST in a Coastal Island of Bangladesh: A Geospatial Approach on St. Martin's Island of Bay of Bengal. Journal of the Indian Society of Remote Sensing. 2021;49(10):2329-2345. doi:10.1007/s12524-021-01389-4
30. Ashikur MR; Rupom RS; Sazzad MH. A remote sensing approach to ascertain spatial and temporal variations of seawater quality parameters in the coastal area of Bay of Bengal; Bangladesh. Remote Sens Appl. 2021;23:100593. doi:https://doi.org/10.1016/j.rsase.2021.100593

31. Chander G; Markham BL; Helder DL. Summary of current radiometric calibration coefficients for Landsat MSS; TM; ETM+; and EO-1 ALI sensors. Remote Sens Environ. 2009;113(5):893-903. doi:10.1016/j.rse.2009.01.007
32. Alam A; Bhat MS; Maheen M. Using Landsat satellite data for assessing the land use and land cover change in Kashmir valley. GeoJournal. 2020;85(6):1529-1543. doi:10.1007/s10708-019-10037-x
33. Cheema MJM; Bastiaanssen WGM. Land use and land cover classification in the irrigated Indus Basin using growth phenology information from satellite data to support water management analysis. Agric Water Manag. 2010;97(10):1541-1552. doi:10.1016/j.agwat.2010.05.009
34. Olofsson P; Foody GM; Stehman S V.; Woodcock CE. Making better use of accuracy data in land change studies: Estimating accuracy and area and quantifying uncertainty using stratified estimation. Remote Sens Environ. 2013;129:122-131. doi:10.1016/j.rse.2012.10.031
35. Adelisardou F; Zhao W; Chow R; Mederly P; Minkina T; Schou JS. Spatiotemporal change detection of carbon storage and sequestration in an arid ecosystem by integrating Google Earth Engine and InVEST (the Jiroft plain; Iran). International Journal of Environmental Science and Technology. 2022;19(7):5929-5944. doi:10.1007/s13762-021-03676-6
36. Sharp. R; Nelson E; Ennaanay D; et al. InVEST User Guide. National Capital Project. Published online 2015.
37. Rahman MdS; Akter S. Carbon Forestry: Scope and Benefit in Bangladesh. Journal of Forest and Environmental Science. 2013;29(4):249-256. doi:10.7747/jfs.2013.29.4.249